J|A|C|S
ARTICLES
Published on Web 12/13/2005

Intramolecularly Sensitized Precipitons: A Model System for Application to Metal Sequestration

Mark R. Ams and Craig S. Wilcox*

Contribution from the Department of Chemistry and The Combinatorial Chemistry Center, University of Pittsburgh, Pittsburgh, Pennsylvania 15260

Received September 6, 2005; E-mail: daylite@pitt.edu

Abstract: We have investigated light-triggered or catalytically activated precipitation agents and have proposed the name "precipiton" for such molecules or molecular fragments. A phase separation is induced when the precipiton isomerizes to a low-solubility form. In this paper we describe the first intramolecularly activated precipitons. The isomerization process is induced by intramolecular triplet energy transfer from a covalently attached metal complex. As expected, intramolecular sensitization leads to a more rapid isomerization than can be achieved by intermolecular sensitization at accessible concentrations. Two isomeric bichromophoric precipiton species, each containing $[Ru(bpy)_3]^{2+}$ and 1,2-bis(biphenyl)ethene units covalently linked together by an ether tether, have been synthesized and characterized, and their photochemical properties have been investigated. The rates of photoisomerization of these complexes, [((*Z*)-1,2-bis(biphenyl)ethene-bpy)Ru(bpy)$_2$](PF$_6$)$_2$ (**2*Z***) and [((*E*)-1,2-bis(biphenyl)ethene-bpy)Ru(bpy)$_2$](PF$_6$)$_2$ (**2*E***), were compared to those of their untethered analogues, (*Z*)-1,2-bis(biphenyl)ethene-OTBS (**1*Z***) and (*E*)-1,2-bis(biphenyl)ethene-OTBS (**1*E***), where ruthenium sensitization occurred through an intermolecular pathway. Upon irradiation with visible light ($\lambda \geq 400$ nm) in degassed solution, **2*Z***/**1*E*** and **1*Z***/**1*E*** obeyed reversible first-order rate kinetics. The intramolecularly sensitized precipiton **2*Z*** isomerized 250 times faster ($k_{2Z\rightarrow 2E} = 1.0 \times 10^{-3}$ s^{-1} with a 51% neutral density filter) than the intermolecular case **1*Z*** ($k_{1Z\rightarrow 1E} = 0.80 \times 10^{-5}$ s^{-1}). For **1*E*** and **2*E***, the isomerization rates were $k_{1E\rightarrow 1Z} = 11.0 \times 10^{-5}$ s^{-1} and $k_{2E\rightarrow 2Z} = 1.6 \times 10^{-3}$ s^{-1}, respectively. The average *Z*/*E* mole ratio at the photostationary state was 62/38 for **2*Z***/**1*E*** and 93/7 for **1*Z***/**1*E***. The impetus for this study was our desire to evaluate the possibility of using metal-binding precipitons that would precipitate only upon metal-to-precipiton binding and would be inert to visible light in the absence of metals.

Introduction

The effective removal of metal contaminants from aqueous and organic media continues to be an important challenge with implications for public health and economic competitiveness.[1] Reducing toxic metal impurities from organic media to the parts per million (ppm) level is required for active pharmaceutical ingredients (APIs), and meeting this need can increase costs for the pharmaceutical industry.[2]

The most common sources of metal contaminants in APIs are the catalysts used in their synthesis. These catalysts are of great importance in reducing the costs of production, and there are no good alternatives that would allow them to be replaced. Commonly observed contaminants are palladium, platinum, ruthenium, and rhodium. Several methods to remove these trace metal impurities have been reported, and all these methods rely on passive equilibrium binding events. For example, silica and synthetic-polymer-derived supports have been used to carry thiol and amine ligands so that expended catalysts, if sufficiently sequestered by these ligating groups, can be removed (scavenged) from a reaction mixture by filtration.[2c,3]

Many pharmaceutical intermediates and final drugs, because of their heterocyclic structures, have good affinities for these metals, a fact that exacerbates the challenge. When a binding agent is used in stoichiometric amounts, in order for such a binding agent or scavenger to be effective at removing a metal impurity, the scavenger ligands must have a much stronger affinity for the metal than the drugs and APIs that are also present. For example, to remove 99% of a contaminant metal from 20 kg of an API, one would need 20 g of a ligand that has a 100 000 times greater affinity for the metal than for the API. Although such ligands can certainly be prepared, their use may be prohibitively expensive.

The challenge can be stated in this way: Given 20 kg of an API or final pharmaceutical containing 1 g of a metal contami-

(1) (a) Kim, S.; Kim, K.; Stuben, D. J. *Environ. Eng.* **2002**, *128*, 705−715. (b) Agrawal, A.; Sahu, K. K.; Pandey, B. D. *Colloids Surf., A* **2004**, *237*, 133−140. (c) Wingenfelder, U.; Hansen, C.; Furrer, G.; Schulin, R. *Environ. Sci. Technol.* **2005**, *39*, 4606−4613. (d) Rahman, M. A.; Ahsan, S.; Kaneco, S.; Katsumata, H.; Suzuki, T.; Ohta, K. *J. Environ. Manage.* **2005**, 107−110.

(2) (a) Rosso, V. W.; Lust, D. A.; Bernot, P. J.; Grosso, J. A.; Modi, S. P.; Rusowicz, A.; Sedergran, T. C.; Simpson, J. H.; Srivastava, S. K.; Humora, M. J.; Anderson, N. G. *Org. Process Res. Dev.* **1997**, *1*, 311−314. (b) Manley, P.; Acemoglu, M.; Marterer, W.; Pachinger, W. *Org. Process Res. Dev.* **2003**, *7*, 436−445. (c) Urawa, Y.; Miyazawa, M.; Ozeki, N.; Ogura, K. *Org. Process Res. Dev.* **2003**, *7*, 191−195.

(3) (a) Brown, J.; Mercier, L.; Pinnavaia, T. J. *Chem. Commun.* **1999**, 69−70. (b) Liu, A. M.; Hidajat, K.; Kawi, S.; Zhao, D. Y. *Chem. Commun.* **2000**, 1145−1146. (c) Nooney, R. I.; Kalyanaraman, M.; Kennedy, G.; Maginn, E. J. *Langmuir* **2001**, *17*, 528−533. (d) Vieira, E. F. S.; Simoni, J. de A.; Airoldi, C. *J. Mater. Chem.* **1997**, *7*, 2249−2252.

10.1021/ja0561340 CCC: $33.50

Scheme 1. An Energy-Activated Precipitation Process To Remove Metal Impurities

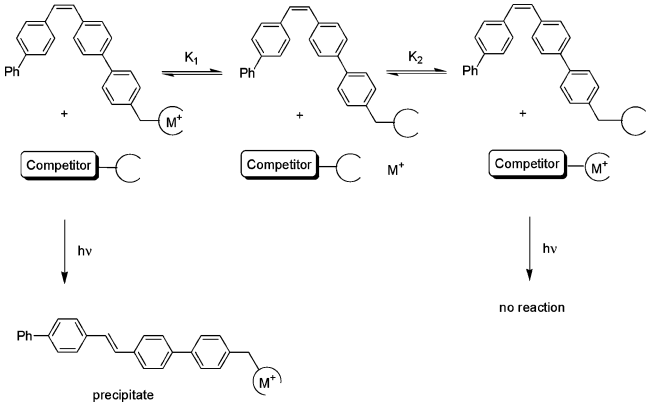

nant (50 ppm), what is the most economical way to reduce this contaminant to less than 5 ppm (a level currently considered acceptable to the industry for the common catalyst-derived contaminants)? Ideally, one would need not more than one molar equivalent of the scavenging ligand, no matter the scale, and this ligand would be recoverable.

We expect that one way in which the problem of ligand competitors in metal scavenging may be overcome is through the use of an energy-driven separation process, wherein the ligated metal would activate isomerization and cause precipitation. In every event that the metal does bind to the precipiton in the *Z* form, if the resulting complex can absorb light, an isomerization process is "triggered" via intramolecular sensitization to produce the *E* isomer. At any time after the point at which the *E* precipiton has reached saturation, the *E* precipiton would precipitate together with the metal, thus decreasing the amount of metal in solution. In short, only a "loaded" ligand will precipitate.[4] The amount of metal bound to scavenger, originally limited by the equilibrium constants for binding to the precipiton ligand (K_1) and competitors (K_2), is increased due to precipitation (Scheme 1). The energy to drive the process is stored in the structure of the scavenging ligand.

In this paper we report on our initial studies of metal complex activated isomerization. A large number of transition metal complexes containing polyimine ligands are capable of visible light absorption and formation of metal-to-ligand charge-transfer (MLCT) triplet states.[5] Within this group, polypyridyl Ru(II) complexes have been widely used as photosensitizers for a variety of reactions, including photoisomerization. In the 1970s, researchers from the Wrighton laboratory demonstrated intermolecular energy transfer from the triplet excited states of Ru(bpy)$_3^{2+}$ complexes to *trans*-stilbene.[6] Since then, intramolecular energy-transfer processes from the ^{3}MLCT state of Ru(II) complexes to stilbene-containing ligands have also been investigated.[7] Studies of related bichromophoric receiver−antenna systems have demonstrated that Ru(bpy)$_3^{2+}$ complexes are capable of intramolecular energy-transfer processes with covalently linked organic chromophores.[8]

Chart 1. Formulas of the Investigated Compounds

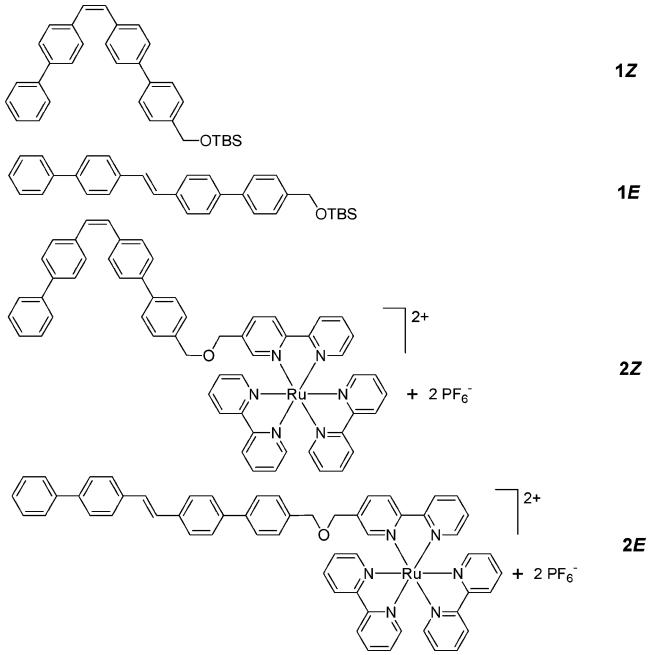

Herein we describe the preparation, photophysical properties, and photoisomerization kinetics of precipitons[9] that are covalently linked and unlinked to a Ru(bpy)$_3^{2+}$ unit. The structures of these compounds are shown in Chart 1. The photoisomerization kinetics at low concentration (10 μM) and photostationary-state ratios of the Ru(II)-linked precipitons **2*Z*/*E*** were compared to those of the unlinked examples **1*Z*/*E***.

Results and Discussion

Synthesis. The preparation of 1,2-bis(biphenyl)ethene TBS ether **1*Z***[9g] and 1,2-bis(biphenyl)ethene alcohol **3*Z***[9d] has been reported previously from our laboratory, and 5-(bromomethyl)-2,2′-bipyridine was synthesized according to a published procedure.[10] The syntheses of **1*E***, **2*Z***, and **2*E*** are summarized in Schemes 2, 3, and 4, respectively.

(4) This requires the right relationship between rates of exchange and precipitation.

(5) (a) Wrighton, M.; Giordano, P. *J. Am. Chem. Soc.* **1979**, *101*, 2888−2897. (b) Sakaki, S.; Okitaka, I.; Ohkubo, K. *Inorg. Chem.* **1984**, *23*, 198−203. (c) Balzani, V.; Juris, A.; Venturi, M. *Chem. Rev.* **1996**, *96*, 759−833. (d) Yam, V.; Chor-Yue, V.; Wu, L. *J. Chem. Soc., Dalton Trans.* **1998**, 1461−1468. (e) Schanze, K. S.; Lucia, L. A.; Cooper, M.; Walters, K. A.; Ji, H.; Sabina, O. *J. Phys. Chem. A* **1998**, *102*, 5577−5584. (f) Vlcek, A. *Coord. Chem. Rev.* **2000**, *200*−*202*, 933−977. (g) Sun, S.; Robson, E.; Dunwoody, N.; Silva, A.; Brinn, I.; Lees, A. J. *Chem. Commun.* **2000**, 201−202. (h) Yam, V. W.; Yang, Y.; Zhang, J.; Chu, W.; Zhu, N. *Organometallics* **2001**, *20*, 4911−4918. (i) Sun, S.; Lees, A. J. *Organometallics* **2002**, *21*, 39−49.

(6) Wrighton, M.; Markham, J. *J. Phys. Chem.* **1973**, *77*, 3042.

(7) (a) Zarnegar, P.; Bock, C. R.; Whitten, D. G. *J. Am. Chem. Soc.* **1973**, *95*, 4367−4372. (b) Shaw, J. R.; Webb, R. T.; Schmehl, R. H. *J. Am. Chem. Soc.* **1990**, *112*, 1117−1123.

(8) (a) Morales, A.; Accorsi, G.; Armaroli, N.; Barigelletti, F.; Pope, S.; Ward, M. D. *Inorg. Chem.* **2002**, *41*, 6711−6719. (b) Wilson, G. J.; Launikonis, A.; Sasse, W. H. F.; Mau, A. W. H. *J. Phys. Chem. A* **1997**, *101*, 4860−4866. (c) Juris, A.; Prodi, L. *New J. Chem.* **2001**, *25*, 1132−1135. (d) Wilson, G. J.; Sasse, W. H. F.; Mau, A. W. H. *Chem. Phys. Lett.* **1996**, *250*, 583−588. (e) Tyson, D.; Bignozzi, C.; Castellano, F. *J. Am. Chem. Soc.* **2002**, *124*, 4562−4563. (f) Tyson, D. S.; Castellano, F. N. *J. Phys. Chem. A* **1999**, *103*, 10955−10960. (g) Wilson, G. J.; Launikonis, A.; Sasse, W. H. F.; Mau, A. W. H. *J. Phys. Chem. A* **1998**, *102*, 5150−5156. (h) Tyson, D. S.; Henbest, K. B.; Bialecki, J.; Castellano, F. N. *J. Phys. Chem. A* **2001**, *105*, 8154−8161. (i) Harriman, A.; Hissler, M.; Khatyr, A.; Ziessel, R. *Chem. Commun*. **1999**, 735−736.

(9) (a) Bosanac, T.; Yang, J.; Wilcox, C. S. *Angew. Chem., Int. Ed*. **2001**, *40*, 1875−1879. (b) Bosanac, T.; Wilcox, C. S. *Chem. Commun*. **2001**, 1618−1619. (c) Bosanac, T.; Wilcox, C. S. *Tetrahedron Lett.* **2001**, *42*, 4309−4212. (d) Bosanac, T.; Wilcox, C. S. *J. Am. Chem. Soc.* **2002**, *124*, 4194. (e) Honigfort, M.; Brittain, W. J.; Bosanac, T.; Wilcox, C. S. *Macromolecules* **2002**, *35*, 4849−4851. (f) Honigfort, M.; Shingtza, L.; Rademacher, J.; Malaba, D.; Bosanac, T.; Wilcox, C. S.; Brittain, W. J. *ACS Symp. Ser.* **2003**, *854*, 250. (g) Bosanac, T.; Wilcox, C. S. *Org. Lett.* **2004**, *6*, 2321−2324.

(10) Ballardini, R.; Balzani, V.; Clemente-Leon, M.; Credi, A.; Gandolfi, M.; Ishow, E.; Perkins, J.; Stoddart, F.; Tseng, H.; Wenger, S. *J. Am. Chem. Soc.* **2002**, *124*, 12786−12796.

Scheme 2. Synthesis of Compound **1*E***

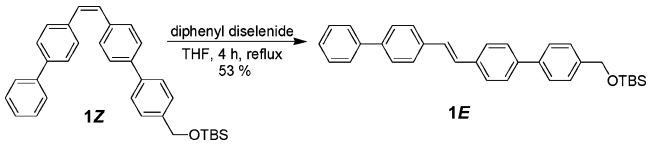

Scheme 3. Synthesis of Ruthenium Complex **2*Z***

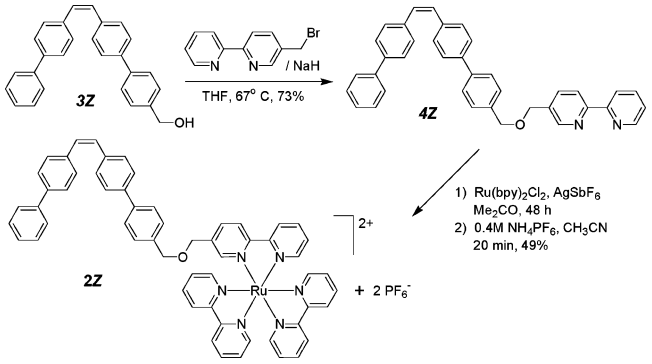

Scheme 4. Synthesis of Ruthenium Complex ***2E***

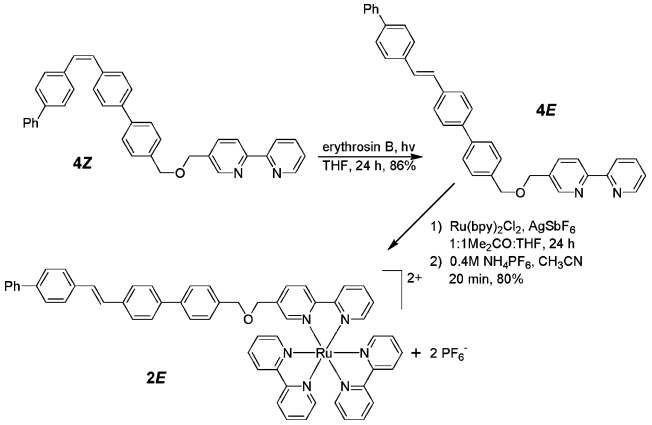

Synthesis of Compound 1*E*. The synthesis of complex **1*E*** is outlined in Scheme 2. Chemical isomerization of TBS ether **1*Z*** with 0.1 equiv of diphenyl diselenide in THF afforded the *E* isomer in 59% yield.

Synthesis of Complex 2*Z*. To begin the preparation of complex **2*Z*** (Scheme 3), alkylation of 1,2-bis(biphenyl)ethene alcohol (**3*Z***) with 5-(bromomethyl)-2,2′-bipyridine afforded a 73% yield of the bipyridine-tagged 1,2-bis(biphenyl)ethene precipiton **4*Z***. The ruthenium complex **2*Z*** was obtained as its bis(hexafluorophosphate) salt in 49% overall yield, after refluxing of *cis*-dichlorobis(2,2′-bipyridine)ruthenium(II) with ligand **4*Z*** in acetone for 48 h and counterion exchange ($NH_4PF_6/H_2O/CH_3CN$).

Synthesis of Complex 2*E*. The synthesis of complex **2*E*** is outlined in Scheme 4. Sensitized isomerization of bipyridine-tagged (*Z*)-1,2-bis(biphenyl)ethene precipiton **4*Z*** with erythrosin B in THF afforded (73%) the *E* isomer **4*E***. The ruthenium complex **2*E*** was obtained as its bis(hexafluorophosphate) salt in 49% overall yield, after refluxing of *cis*-dichlorobis(2,2′-bipyridine)ruthenium(II) with ligand **4*E*** in 1:1 acetone:THF followed by counterion exchange ($NH_4PF_6/H_2O/CH_3CN$). It was observed that **2*E*** and **2*Z*** quickly interconvert under normal room illumination. Therefore, operations with pure isomers were carried out under red light.

Table 1. Spectroscopic and Photophysical Data (CH_3CN, 298 K)

compound	absorption λ_{max}/nm (ϵ/M^{-1} cm^{-1})	emission λ_{max}/nm
1*Z*	265 (61 500), 309 (44 300)	
1*E* [c]	335 (59 300)	
2*Z*	247 (30 122), 286 (198 400), 341 (33 100), 450 (18 260)	612 [a]
2*E*	245 (66 757), 286 (178 080), 341 (59 300), 450 (10 755)	612 [a]
$Ru(bpy)_3^{2+}$	288 (57 400), 450 (10 500)	613 [a]
3*Z*	268 (31 000), 331 (31 600)	315 [b]
4*Z*	274 (34 200), 290 (33 200), 330 (24 800)	

[a] λ_{exc} = 450 nm. [b] λ_{exc} = 285 nm. [c] Measured in CH_2Cl_2 at 298 K.

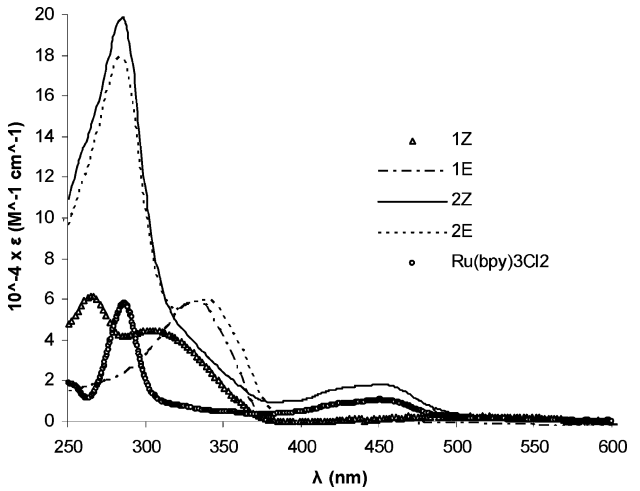

Figure 1. Room-temperature absorption spectra recorded for degassed 10 μM acetonitrile solutions of **1*Z***, **1*E*** (performed in CH_2Cl_2), **2*Z***, **2*E***, and $Ru(bpy)_3^{2+}$.

Absorption and Emission Spectroscopy. The photophysical data for these new compounds are summarized in Table 1. Figure 1 shows the absorption spectra for **1*Z***, **1*E***, **2*Z***, **2*E***, and $Ru(bpy)_3Cl_2$ at room temperature. Compounds **2*Z***, **2*E***, and $Ru(bpy)_3Cl_2$ were dissolved in neat acetonitrile, while **1*E*** had to be dissolved in neat CH_2Cl_2. Comparison of the absorption profiles displayed in this figure allows the following assignments to be made. Complexes **2*E*** and **2*Z*** are essentially composed of 1,2-bis(biphenyl)ethene TBS ether **1*Z*/*E*** appended to a $Ru(bpy)_3^{2+}$ moiety. With reference to previous work on similar systems, the band maximum at 450 nm is tentatively assigned as the MLCT (Ru → bpy) transition, as shown in the same region for $Ru(bpy)_3^{2+}$.[8a] The features in the 270−300 nm spectroscopic region are those of bpy-centered $\pi \rightarrow \pi^*$ transitions. The absorption characteristics in the region 260−370 nm are identified as being of phenylene origin and are ascribed to population of the ^{1}phenylene excited state.[11] Absorption in the region 321−377 nm, which is seen to be most intense for the trans isomer **2*E***, is attributed to the $\pi \rightarrow \pi^*$ transition localized on the ethylene functionality for each precipiton. The absorption spectra of Figure 1 indicate that absorption results from additive properties of scarcely interacting Ru-based and 1,2-bis(biphenyl)ethene chromophores. This is consistent with the expectation that the ether linkage provides for electronic separation between the Ru and 1,2-bis(biphenyl)ethene photo-

(11) Crews, P.; Rodriguez, J.; Jaspars, M. Optical and Chiroptical Techniques: Ultraviolet Spectroscopy. In *Organic Structure Analysis*; Houk, K. N., Loudon, G. M., Eds.; Topics in Organic Chemistry Series; Oxford University Press: New York, 1998; pp 349−373.

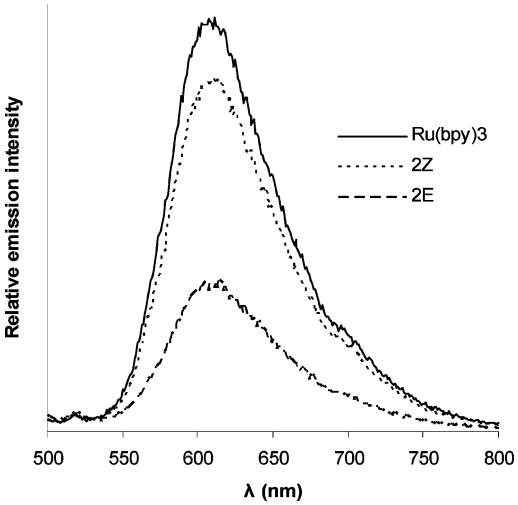

Figure 2. Room-temperature emission spectra recorded for degassed 10 μM acetonitrile solutions of complexes **2*Z***, **2*E***, and $Ru(bpy)_3Cl_2$.

active units. From the absorption properties of **2*Z***, **2*E***, and their components, it seems reasonable that the use of $\lambda_{exc} \geq 400$ nm irradiation would result in selective excitation of the $Ru(bpy)_3^{2+}$ chromophore. Conversely, use of $\lambda_{exc} \leq 370$ nm irradiation would produce excited states of both Ru and 1,2-bis(biphenyl)-ethene components.

Excitation of complexes **2*Z*** and **2*E*** at $\lambda_{exc} = 450$ nm in acetonitrile at room temperature results in luminescence centered at 570−680 nm. The data are summarized in Table 1, and Figure 2 shows the excitation spectra of **2*Z***, **2*E***, and $Ru(bpy)_3^{2+}$. The spectra exhibit overlapping profiles, with the band maxima peaking at 612 nm. The emission intensity for the cis isomer is shown to be approximately 2.5 orders of magnitude more intense than that of the trans isomer and slightly red-shifted, by 3 nm. It is known for stilbene that the triplet-state energy for the cis isomer (63 kcal/mol) is higher than that for the trans isomer (49 kcal/mol).[12] In the case of **2*E***, it is likely that the triplet energy from the ^{3}MLCT excited state of $Ru(bpy)_3^{2+}$ (49 kcal/mol) is favorably intramolecularly transferred to the *trans*-alkene moiety as a deactivation pathway. For the cis isomer **2*Z***, on the other hand, such an intramolecular process is disfavored due to the higher triplet-state energy of the cis isomer.[5d]

Photoisomerization Reactivity in O_2-Free Solution

Electronic Absorption Studies. For compounds **1*Z*/*E*** and **2*Z*/*E***, direct visible light excitation at $\lambda \geq 400$ nm gave cis ↔ trans isomerization as the only observed photoreaction event. To determine if **2*Z*/*E*** isomerizes under these conditions primarily due to an intramolecular interaction with the bound $Ru(bpy)_3^{2+}$ sensitizer, the concentration was varied and the photoreactivity of analogue **1*Z*/*E*** with $Ru(bpy)_3^{2+}$ was studied for comparison. At dilute concentrations (≤10 μM), intermolecular quenching processes between donor and acceptor can be reduced so that the observed quenching is primarily due to intercomponent interactions.[13]

A 10 μM degassed solution of **1*Z*/*E*** in 70:30 THF:CH_3CN was irradiated in a darkened room using a 25-W incandescent lamp equipped with a 400-nm cutoff filter. UV−vis spectral changes with a clean and well-defined isosbestic point were observed. The isomerizations were expectedly slow, requiring over 9 h to give no further UV−vis spectroscopic changes. For **1*E***, we observed an isosbestic point at 304 nm (Figure 3).

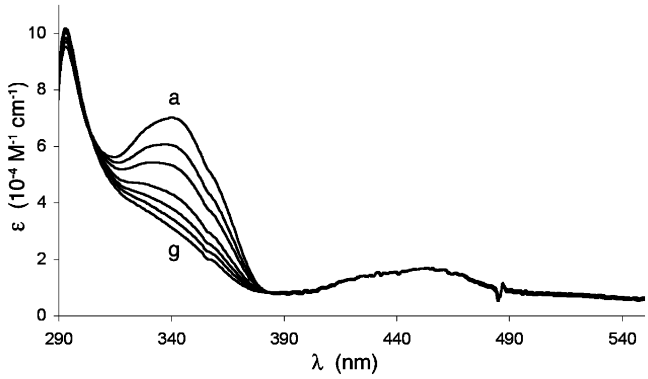

Figure 3. UV−vis spectral changes observed with complex **1*E*** upon irradiation at $\lambda \geq 400$ nm at 0, 50, 100, 210, 300, 410, and 565 min (a−g, respectively) in 10 μM 70:30 THF:CH_3CN.

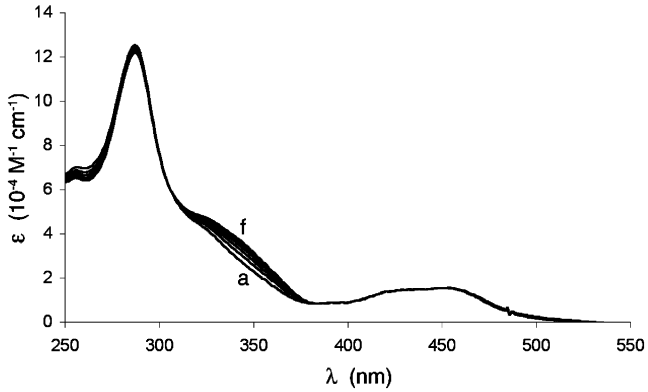

Figure 4. UV−vis spectral changes observed with complex **2*Z*** (8.2 μM in degassed acetonitrile) upon irradiation at $\lambda \geq 400$ nm at 0, 20, 40, 60, 80, and 100 min (a−f, respectively).

From initial photoisomerization experiments with **2*Z*/*E***, we learned that the reaction rate was too rapid for direct observation under the conditions used for **1*Z*/*E***. To slow the reaction rate, the light intensity was reduced by 51% through equipping the lamp with a neutral density filter. Upon irradiation of a degassed acetonitrile solution of **2*Z*** (8.2 μM) or **2*E*** (7.4 μM), UV−vis spectral changes with a clean and well-defined isosbestic point were observed. Complex **2*Z*** showed an increase in absorption intensity at 341 nm as well as an isosbestic point at 305 nm (Figure 4). Complex **2*E*** showed a decrease in absorption intensity at 341 nm as well as an isosbestic point at 303 nm (Figure 5). The photostationary state was reached within 45 min. The isomers **2*Z*/*E*** are distinguishable by ^{1}H NMR spectroscopy due to the chemical shift differences of the alkene and methylene protons. Observation of the changes in NMR chemical shift and peak intensity of **2*Z*/*E*** during photoisomerization confirmed that the UV−vis spectroscopic changes are associated with the isomerization of the carbon−carbon double bond.

Kinetics. To further investigate the process occurring in complexes **2*Z*/*E*** and compounds **1*Z*/*E***, quantitative rate studies were undertaken. Solutions of pure **1*Z*** and **1*E*** (10 μM, 70:30 THF:CH_3CN) were irradiated at $\lambda \geq 400$ nm in the presence of 10 μM $Ru(bpy)_3^{2+}$ sensitizer and monitored by UV−vis at 350 nm. The concentration of cis and trans precipiton present is

(12) Saltiel, J.; Marchland, G.; Kaminska, E.; Smothers, W.; Meuller, W.; Charlton, J. *J. Am. Chem. Soc.* **1984**, *106*, 3144.
(13) Schlicke, B.; Belser, P.; De Cola, L.; Sabbioni, E.; Balzani, V. *J. Am. Chem. Soc.* **1999**, *121*, 4207.

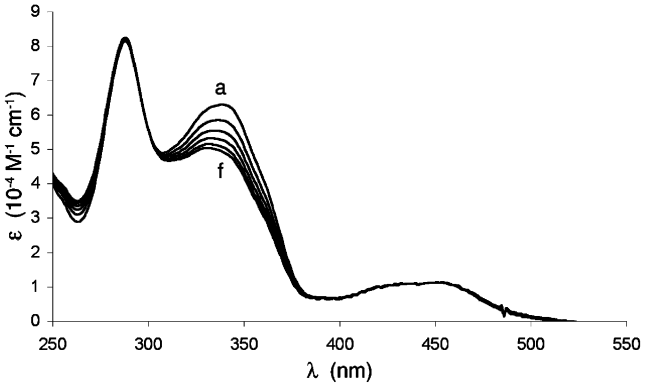

Figure 5. UV−vis spectral changes observed with complex **2*E*** (7.4 μM in degassed acetonitrile) upon irradiation at $\lambda \geq 400$ nm at 0, 20, 40, 60, 80, and 100 min (a−f, respectively).

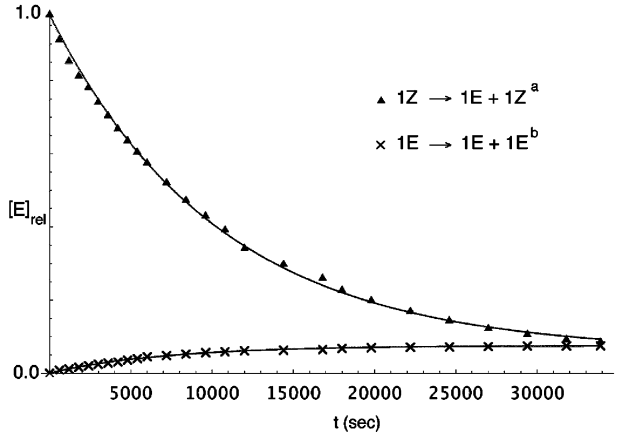

Figure 6. Photochemical production of photostationary state concentrations upon irradiation at $\lambda \geq 400$ nm of **1*Z***/***E*** starting from pure **1*Z***.

Table 2. Isomerization Rate Constants and Photostationary State Ratios for the Photoisomerization Process of **1*Z***/***E*** and **2*Z***/***E*** upon Irradiation at $\lambda \geq 400$ nm

reaction	$k\,(s^{-1}) \times 10^3$	*Z*/*E* average ratio
1*Z* → **1*E***	0.0080	93/7
1*E* → **1*Z***	0.11	
2*Z* → **2*E***	1.0	62/38
2*E* → **2*Z***	1.6	

plotted as a function of irradiation time in Figure 6. After 9.4 h of irradiation, solutions containing each pure isomer came to a final *Z*/*E* photostationary state, the average ratio of which was determined to be 93/7. The plots fit well to a reversible first-order rate curve (see Figure 6), and the rate constants were determined to be $k_{Z\rightarrow E} = 0.80 \times 10^{-5}$ s^{-1} and $k_{E\rightarrow Z} = 11.0 \times 10^{-5}$ s^{-1} (Table 2).

Solutions of **2*Z*** and **2*E*** (CH_3CN) were irradiated under the same conditions[14] as **1*Z***/***E*** and came to a final *Z*/*E* photostationary state, the average ratio of which was determined to be 62/38. Figure 7 plots the relative concentration of **2*Z***/***E*** formed or depleted in each reaction as a function of time.[15] The plots fit well to a reversible first-order rate curve, and the rate

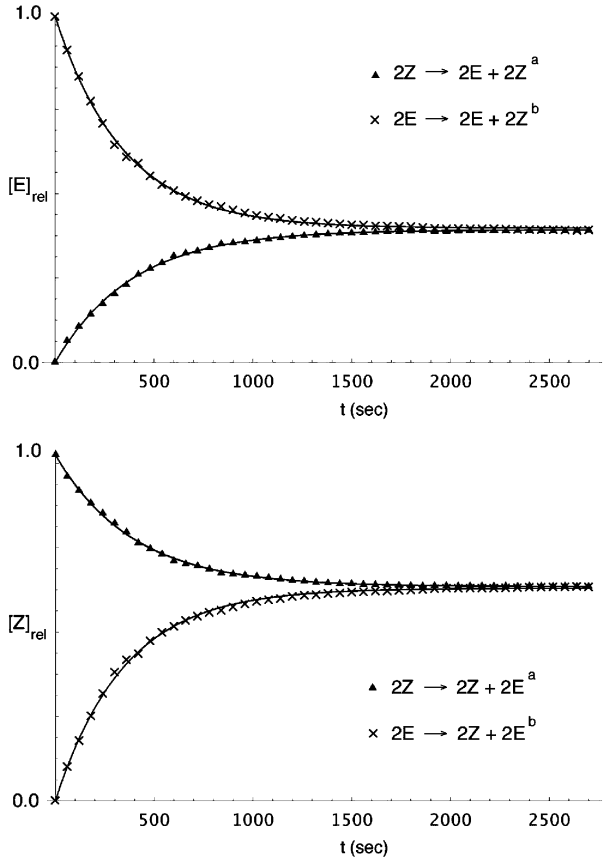

Figure 7. Photochemical production of photostationary state concentrations upon irradiation at $\lambda \geq 400$ nm of **2*Z*** → **2*E*** and **2*E*** → **2*Z***. (Top) [**2*E***] vs time. (Bottom) [**2*Z***] vs time. [a][*Z*] vs time starting with 8.2 μM **2*Z***. [b][*E*] vs time starting with 7.2 μM **2*E***.

constants were determined to be $k_{Z\rightarrow E} = 1.0 \times 10^{-3}$ s^{-1} and $k_{E\rightarrow Z} = 1.6 \times 10^{-3}$ s^{-1}. When factoring in the light reduction due to the 51% neutral density filter, the rate constant for cis → trans isomerization for **2*Z*** is 250 times faster than for **1*Z***, and the trans → cis isomerization for **2*E*** is 29 times faster than for **1*E***.

A control experiment to correct for the presence of any background cis ↔ trans isomerization occurring from simple exposure to direct irradiation was performed on the untethered precipiton **3*Z***. A 20 mM solution of **3*Z*** in acetonitrile was prepared and irradiated at $\lambda \geq 400$ nm for 1 h. Only 3% had isomerized, as determined by ^{1}H NMR spectroscopy analysis, and produced a small amount of white precipitate. Formation of the trans isomer, however, was not observable by NMR due to its high insolubility.

Conclusions

We have synthesized and characterized two new stilbene-based precipitons, **2*Z*** and **2*E***, both featuring a covalently bound $Ru(bpy)_3^{2+}$ sensitizer. Upon irradiation at visible wavelengths ($\lambda \geq 400$ nm), the complexes undergo photoisomerization. The process was monitored by electronic absorption and ^{1}H NMR spectroscopy. The reversible first-order rate constants for **2*Z***/***E*** have been determined and compared to those of the intermolecularly sensitized untethered analogues **1*Z***/***E***. At low concentration (≤ 10 μM), **2*Z*** isomerized 250 times faster than **1*Z*** + $Ru(bpy)_3^{2+}$. Each isomer came to a final *Z*/*E* photostationary state, the average ratio of which was determined to be 62/38

(14) The irradiation light, however, was reduced 51% using a neutral density filter.

(15) ^{1}H NMR spectroscopy and elemental analysis of **2*E*** revealed that 12% of **4*E*** was present in the sample prior to irradiation. To account for this, the absorbance due to **4*E*** was subtracted from the observed absorbance. The correction simply displaces curve and has no affect on the derived rate constants.

for **2*Z*** → **2*E*** and 93/7 for **1*Z*** → **1*E***. In this model study we have been able to demonstrate a significant isomerization rate enhancement for precipitons containing a bound metal sensitizer compared to their unbound analogues. This is a significant step forward in the development of precipitons as energy-driven metal scavengers.

Experimental Section

General Synthetic Methods. The complexes $Ru(bpy)_2Cl_2$ and $Ru(bpy)_3Cl_2$ were purchased from Strem Chemicals Inc. and used as received. All other starting materials were purchased from Aldrich Chemical Co. and were used as received. Preparation and purification of the complexes **2*Z*** and **2*E*** were conducted in a darkened laboratory under red light illumination.

(*E*)-4′-(2-Biphenyl-4-yl-vinyl)-biphenyl-4-ylmethoxy-*tert*-butyl-dimethyl-silane (1*E*). A solution of TBS ether **1*Z***[9g] (175 mg, 368 μmol) and diphenyl diselenide (12 mg, 37 μmol) in THF (1.5 mL) was heated at reflux for 4 h. The solution was cooled to 23 °C, and volatile components of the reaction mixture were removed in vacuo. The crude solid was triturated with Et_2O (4 mL), filtered, and washed with Et_2O (2 × 2 mL). The volatile components of the filtrate were removed in vacuo, and the crude solid was triturated with hexanes (3 × 3 mL) and filtered. Solids were collected to afford TBS ether **1*E*** as a white crystalline solid (93 mg, 53%): R_f 0.44 (9:1 Hex:EtOAC); mp 260 °C; IR (KBr) 2949, 2927, 2854, 1495, 1471, 1462, 1408, 1378, 1252, 1089, 1062, 973, 835, cm^{-1}; UV−vis (CH_2Cl_2, 10 μM) λ_{max} 335 nm, ϵ 59 300 M^{-1} cm^{-1}; ^{1}H NMR (300 MHz, $CDCl_3$) δ 7.66−7.60 (m, 12H), 7.49−7.33 (m, 5H), 7.20 (s, 2H), 4.81 (s, 2H), 0.98 (s, 9H), 0.14 (s, 6H); ^{13}C NMR, too insoluble to obtain; HRMS *m*/*e* calcd for $C_{33}H_{36}OSi$ 476.2535, found 476.2515.

(*Z*)-5-[4′-(2-Biphenyl-4-yl-vinyl)-biphenyl-4-ylmethoxymethyl]-[2,2′]bipyridine (4*Z*). To a cooled solution (0 °C) of benzyl alcohol **3*Z***[9d] (500 mg, 1.38 mmol) in THF (138 mL) was added dry NaH (66.2 mg, 2.76 mmol). The solution was warmed to 23 °C and stirred for 2 h. 5-(Bromomethyl)-2,2′-bipyridine (354 mg, 1.42 mmol) was then added, and the solution was stirred for 2 h at 23 °C and then heated at reflux for 17.5 h. The solution was cooled to 23 °C, and volatile components of the reaction mixture were removed in vacuo. The crude solid was combined with H_2O (300 mL), and the solution was extracted with CH_2Cl_2 (3 × 300 mL). The combined organic phases were washed with brine (900 mL), dried with $MgSO_4$, and filtered. Volatile components in the filtrate were removed in vacuo, and the residue was purified by flash chromatography (SiO_2, CH_2Cl_2 then 99:1 CH_2Cl_2:MeOH) to afford **4*Z*** as a pale green solid (537 mg, 73%): R_f 0.31 (CH_2Cl_2); mp 113−115 °C; IR (KBr) 3030, 3003, 2857, 1598, 1588, 1557, 1460,1395, 1353, 1088, 881, 815; UV−vis (CH_3CN, 10 μM) λ_{max} 274 nm, ϵ 34 200 M^{-1} cm^{-1}, 290 nm, ϵ 33 200 M^{-1} cm^{-1}, 330 nm, ϵ 24 800 M^{-1} cm^{-1}; ^{1}H NMR (300 MHz, CD_3CN) δ 8.69−8.66 (m, 2H), 8.43−8.41 (app d, J = 8 Hz, 2H), 7.95−7.90 (m, 2H), 7.72−7.63 (m, 5H), 7.56 (app d, J = 7 Hz, 4H), 7.46 (app d, J = 8.5 Hz, 4H), 7.42 (app s, 1H), 7.34 (app d, J = 8 Hz, 4H), 6.72 (s, 2H), 4.67 (s, 2H), 4.65 (s, 2H); ^{13}C NMR (75 MHz, CD_3CN) δ 156.1, 156.8, 149.3, 148.8, 140.8, 140.4, 140.0, 139.6, 137.0, 136.6, 136.5, 136.4, 130.2, 130.1, 129.6, 129.5, 129.8, 128.4, 127.4, 127.1, 127.0, 126.9, 124.0, 121.2, 121.0, 72.3, 69.6; HRMS(EI) *m*/*z* calcd for $C_{38}H_{30}N_2O$ 530.2358, found 530.2383.

(*E*)-5-[4′-(2-Biphenyl-4-yl-vinyl)-biphenyl-4-ylmethoxymethyl]-[2,2′]bipyridine (4*E*). A solution of bipyridine **4*Z*** (227 mg, 0.428 mmol) and erythrosine B (17.0 mg, 0.0214 mmol) in THF (4.28 mL) was stirred and irradiated with a 250-W incandescent lamp for 21 h. The solution was cooled to 0 °C, paper filtered, and washed with cold THF (4 × 10 mL) to afford **4*E*** as a yellow solid (173.4 mg, 87%): mp 300−310 °C; IR (KBr) 3048, 3030, 2855, 1911, 1589, 1557, 1496, 1461, 1436, 1397, 1357, 1081, 970, 832, 807, 795, 763, 752, 742, 731, 691; ^{1}H NMR (300 MHz, $CDCl_3$) δ 8.75−8.69 (m, 2H), 8.46 (app d, J = 8 Hz, 2H), 7.90 (dd, J = 8, 2 Hz, 1H), 7.85 (dd, J = 8, 2 Hz, 1H), 7.66−7.62 (m, 12H), 7.50 (app d, J = 9 Hz, 3H), 7.43 (app s, 1H), 7.38−7.34 (m, 2H), 7.20 (s, 2H), 4.68 (s, 2H), 4.67 (s, 2H); ^{13}C NMR, too insoluble to obtain; HRMS(EI) *m*/*z* calcd for $C_{38}H_{31}N_2O$ [M + H] 531.2436, found 531.2452.

(*Z*)-[5-(4′-(2-Biphenyl-4-yl-vinyl)-biphenyl-4-ylmethoxymethyl]-[2,2′]bipyridine]-bis(2,2′-bipyridine)ruthenium(II) Bis(hexafluorophosphate) (2*Z*). A solution of *cis*-dichlorobis(2,2′-bipyridine)ruthenium-(II) dihydrate (90.8 mg, 0.188 mmol) and silver hexafluoroantimonate(V) (132 mg, 0.376 mmol) in acetone (12.5 mL) under N_2 was heated at reflux for 48 h, followed by filtration of AgCl. Bipyridine **4*Z*** (99.8 mg, 0.188 mmol) was added to the filtrate, and the mixture was heated at reflux for 24 h. Volatile components of the reaction mixture were removed in vacuo to afford a crude red solid that was purified by flash chromatography (SiO_2, 19:1 CH_3CN:0.4 M KNO_3(aq)). The desired fractions were combined, and volatile components were reduced in volume to 25 mL. The solution was combined with 0.25 M NH_4PF_6-(aq) (10 mL), stirred at 23 °C for 20 min, and then extracted with $CHCl_3$ (3 × 100 mL). The organic extract was washed with H_2O (2 × 200 mL). Volatile components of the organic layer were removed in vacuo to afford complex **2*Z*** as a red solid (114 mg, 49%): R_f 0.16 (19:1 CH_3CN:0.4 M KNO_3(aq) on pretreated silica); mp 164−166 °C; IR (KBr) 3027, 2919, 2853, 1603, 1464, 1446, 1093, 838, 761, 730, 699; UV−vis (CH_3CN, 10 μM) λ_{max} 247 nm, ϵ 30 122 M^{-1} cm^{-1}, 286 nm, ϵ 198 400 M^{-1} cm^{-1}, 341 nm, ϵ 33 100 M^{-1} cm^{-1}, 450 nm, ϵ 10 755 M^{-1} cm^{-1}; ^{1}H NMR (300 MHz, CD_3CN) δ 8.49−8.46 (m, 4H), 8.44−8.39 (m, 2H), 8.06−8.01 (app t, J = 15, 8 Hz, 4H), 7.97 (dd, J = 5, 2 Hz, 1H), 7.92 (dd, J = 8, 1 Hz, 1H), 7.73−7.69 (m, 5H), 7.65−7.60 (m, 6H), 7.58−7.55 (m, 3H), 7.47−7.45 (m, 2H), 7.42−7.34 (m, 9H), 7.33−7.27 (m, 1H), 7.23 (app d, J = 8, 2 Hz, 2H), 6.74 (s, 2H), 4.51 (ABq, J = 14 Hz, 2H), 4.47 (s, 2H); ^{13}C NMR (75 MHz, CD_3-CN) δ 158.5, 158.4, 158.3, 157.4, 153.1, 153.0, 150.9,141.7, 141.2, 141.0, 140.8, 140.6, 139.3, 139.2, 138.7, 138.1, 138.0, 137.7, 131.5, 131.4, 130.9, 130.8, 130.3, 129.8, 129.7, 129.6, 129.07, 129.04, 129.01, 128.97, 128.94, 128.90, 128.90, 128.2, 128.1, 125.7, 125.6, 125.5, 125.3, 73.6, 69.6; HRMS(ES) *m*/*z* calcd for $C_{58}H_{46}F_6N_6OPRu$ [M − PF_6]$^+$ 1089.2418, found 1089.2452, 944.14 [M − 2PF_6]$^+$. Anal. Calcd: C, 56.45; H, 3.76; Ru, 8.19. Found: C, 56.55; H, 3.74; Ru, 7.22.

(*E*)-[5-(4′-(2-Biphenyl-4-yl-vinyl)-biphenyl-4-ylmethoxymethyl]-[2,2′]bipyridine]-bis(2,2′-bipyridine)ruthenium(II) Bis(hexafluorophosphate) (2*E*). A solution of *cis*-dichlorobis(2,2′-bipyridine)ruthenium-(II) dihydrate (183 mg, 0.377 mmol) and silver hexafluoroantimonate(V) (259 mg, 0.754 mmol) in acetone (8 mL) under N_2 was stirred at 23 °C for 72 h, followed by filtration of AgCl. Bipyridine **4*E*** (200 mg, 0.377 mmol) was added to the filtrate and diluted with acetone (4 mL)/THF (12 mL). The mixture was heated at reflux for 28 h. The solvent was removed under reduced pressure, and the crude product was dissolved in CH_3CN (10 mL). Next, 0.25 M NH_4PF_6(aq) (10 mL) was added, and the mixture was stirred at 23 °C for 30 min. The solution was then extracted into CH_2Cl_2 (3 × 200 mL) and washed with H_2O (200 mL). Volatile components of the organic layer were removed in vacuo to afford a red solid. The solid was dissolved in CH_3CN (125 mL) and precipitated with diethyl ether (100 mL). The resulting precipitate was filtered to afford complex **2*E*** as a red solid (46.5 mg, 80%): R_f 0.84 (19:1 CH_3CN:0.4 M KNO_3(aq) on pretreated silica); UV−vis (CH_3CN, 10 μM) λ_{max} 245 nm, ϵ 66 757 M^{-1} cm^{-1}, 286 nm, ϵ 178 080 M^{-1} cm^{-1}, 341 nm, ϵ 59 300 M^{-1} cm^{-1}, 450 nm, ϵ 10 755 M^{-1} cm^{-1}; ^{1}H NMR (300 MHz, CD_3CN) 8.50−8.42 (m, 6H), 8.07−7.99 (m, 4H), 7.99−7.93 (m, 2H), 7.80−7.60 (m, 16H), 7.57−7.54 (m, 1H), 7.54−7.44 (m, 2H), 7.44−7.30 (m, 9H), 7.26 (d, J = 8 Hz, 2H), 4.58−4.50 (m, 2H), 4.50−4.44 (m, 2H); ^{13}C NMR (151 MHz, CD_3CN) δ 157.97, 157.94, 157.90, 156.9, 152.72, 152.66, 152.63, 150.4, 141.26, 141.12, 140.82, 140.49, 140.31, 138.80, 138.79, 138.17, 137.85, 137.59, 137.17, 129.95, 129.28, 129.22, 129.04, 128.60, 128.56, 128.49,128.42, 128.25, 128.22, 128.09, 128.04, 127.70, 125.25, 125.13, 124.85, 73.09, 69.12; HRMS(ES) *m*/*z* calcd for $C_{58}H_{46}F_6N_6OPRu$ [M

$- PF_6]^+$ 1089.2418, found 1089.2368. Anal. Calcd: C, 56.45; H, 3.76; Ru, 8.19. Found: C, 57.64; H, 3.94; Ru, 7.23.

Photochemical Experiments. All of the measurements were performed at room temperature in degassed CH_3CN or THF/CH_3CN (70:30) solutions. UV−vis absorption spectra were recorded with an Agilent 8453 spectrophotometer. Photoisomerization experiments were monitored by recording the UV−vis absorption of **2*Z*/*E*** and **1*Z*/*E*** at 341 nm (exclusively) with a PerkinElmer Lambda 9 UV−vis spectrometer. All experiments were performed in the dark or under red light due to the high sensitivity of the compounds to normal ambient lighting. Uncorrected luminescence spectra were recorded with a Cary Eclipse fluorescence spectrometer equipped with Varian software. The excitation light used for all photoisomerization experiments was produced by a 25-W Bausch & Lomb microscope lamp positioned 5 cm from the sample. The light emitted was filtered by using a cutoff filter ($\lambda \leq$ 400 nm).

Acknowledgment. Financial support from the National Institute of General Medical Sciences is gratefully acknowledged. The authors would also like to recognize the help of Prof. Stephane Petoud, Prof. Dave Waldeck, and Ms. Demetra Chengelis in acquiring the absorption spectra.

Supporting Information Available: Experimental details, ^1H and ^{13}C NMR spectra, and complete characterization data for all compounds. This material is available free of charge via the Internet at http://pubs.acs.org.

JA0561340